

Oxidation Leading to Reduction: Redox-Induced Electron Transfer (RIET)

Joel S. Miller* and Kil Sik Min

electron transfer · magnetic properties ·
mixed-valent compounds · redox chemistry ·
valence ambiguity

In Memory of Alan G. MacDiarmid

Complex electron transfer reactions have been characterized whereby in addition to electron transfer, subsequent electrochemical, chemical and even in some cases biological consequences occur. These include a secondary electron transfer that leads to a major rearrangement of the electronic structure, such that an initial oxidation leads to a reduction (or an initial reduction leads to an oxidation) for these valence ambiguous compounds. Mixed valency and valence-tautomeric behaviors can additionally result from these complex electron-transfer-induced reactions.

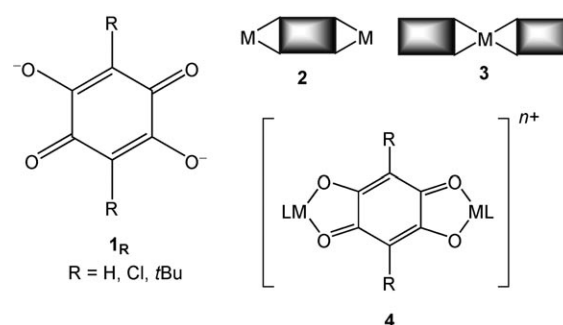
1. Introduction

Electron transfer reactions are a crucial realm of chemistry with important ramifications in biology, physics, and materials. The number of such reactions are so voluminous that reviews are inadequate, and compendiums and encyclopedias are required.^[1] Addition of an electron constitutes reduction, while loss of an electron is oxidation. To conserve electrons these events occur in tandem and are referred to as reduction–oxidation, or redox, reactions. The study of the rates and/or consequences of these reactions has been an important aspect of chemistry for a long time and continues to be at the forefront of contemporary research with a multitude of important fundamental, interdisciplinary, and technological implications.

Recently we uncovered a reaction whereby a one-electron oxidation led to a one-electron reduction occurring. While this would appear to be a play on words, a semantic expose, hype, or an oxymoron, the reality is sound science arising from complex multi-electron transfers whereby oxidation

leads to reduction. In fact, other examples of redox-induced electron transfer (RIET) reactions, as well as related phenomena, have been documented, and collectively are the basis of this Minireview.

Complexes that exhibit RIET possess one or more redox-active ligands that can be isolated in several oxidation states. Such redox-active ligands are frequently referred to as being non-innocent.^[2] A common example is a tetraoxolene dianion (or anilate) **1_R**, and its different redox forms **1_R^{n−}** (*n* = 0, 1, 2,

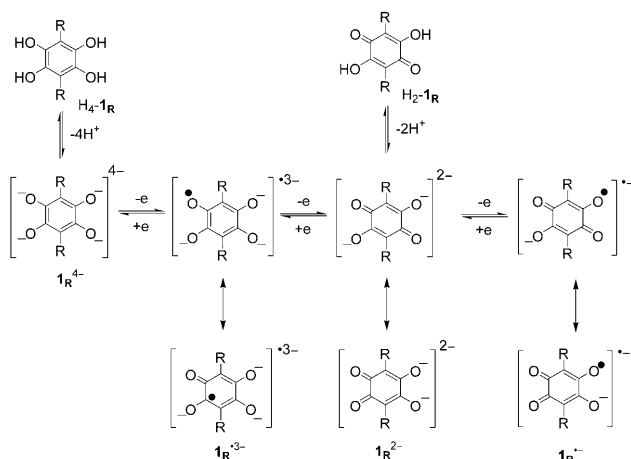


3, 4) are described in Scheme 1. Dianion **1_R** can bridge two redox-active metal ions, that is, form a dinuclear metal complex, as schematically illustrated as **2**. RIET also has been recently established for a mononuclear metal complex with more than one chelating non-innocent ligand, as schematically illustrated as **3**. Note, that as illustrated for a chromium-based mononuclear metal complex discussed in Section 4, the characterization of RIET occurring can be fraught with challenges.

The most studied system has the generic composition of **[LM1_RML]ⁿ⁺**, **4**, where M is typically Cr, Fe, or Co bridged by

[*] Prof. Dr. J. S. Miller
Department of Chemistry
University of Utah
Salt Lake City, UT 84112-0850 (USA)
Fax: (+1) 801-581-8433
E-mail: jsmiller@chem.utah.edu
Homepage: <http://www.chem.utah.edu/directory/faculty/miller.html>

Dr. K. S. Min
Department of Chemistry Education
Kyungpook National University
Daegu, 702-701 (Republic of Korea)



Scheme 1.

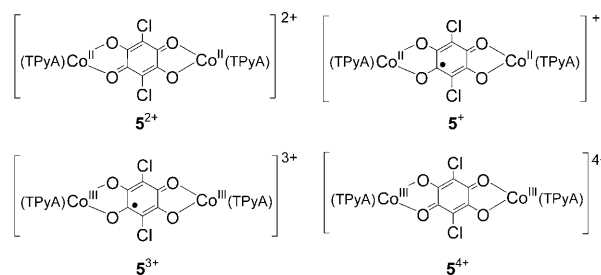
$\mathbf{1}_R^{n-}$, and L is a tetradentate (or two bidentate) capping ancillary ligand.

2. Dinuclear Tetraoxolate Complexes

Several dinuclear metal complexes possessing the bridging tetraoxolate ligands, typified by 1,4-dichlorotetraoxolate, or more commonly chloranilate ($\mathbf{1}_R^{2-}$; $R = \text{Cl}$), **4**, support complex electron-transfer chemistry that involves reduction of the ligand in addition to oxidation of the metal sites. In addition to valence tautomers and mixed-valent materials, transitions from valence RIET-induced tautomers to mixed-valent materials have been observed.

2.1. Dinuclear Cobalt Complexes

With the objective making the mixed valent $\text{Co}^{\text{III}}\mathbf{1}_{\text{Cl}}^{2-}\text{Co}^{\text{II}}$ -containing species, oxidation of $[\text{TPyACo}^{\text{II}}(\mathbf{1}_{\text{Cl}}^{2-})\text{Co}^{\text{II}}\text{TPyA}](\text{BF}_4)_2$ [$\text{TPyA} = \text{tris}(2\text{-pyridylmethyl})\text{amine}$] ($\mathbf{5}^{2+}$) by the ferrocenium ion formed $\mathbf{5}^{3+}$, but its electronic structure and magnetic behavior were inconsistent with the targeted mixed-valent $[\text{TPyACo}^{\text{III}}(\mathbf{1}_{\text{Cl}}^{3-})\text{Co}^{\text{II}}\text{TPyA}]^{3+} \leftrightarrow [\text{TPyACo}^{\text{II}}(\mathbf{1}_{\text{Cl}}^{2-})\text{Co}^{\text{III}}\text{TPyA}]^{3+}$ ($\mathbf{5}^{3+}$), which should possess one $S = 3/2$ Co^{II} site.^[3] The magnetic behavior instead was characteristic of



an $S = 1/2$ system and $\mathbf{5}^{3+}$ was described as $[\text{TPyACo}^{\text{III}}(\mathbf{1}_{\text{Cl}}^{3-})\text{Co}^{\text{III}}\text{TPyA}]^{3+}$. This was confirmed from its EPR spectrum and a detailed analysis of the ν_{CO} IR absorptions as well as Co–O, C–O, and C–C bond lengths. Further oxidation formed diamagnetic ($S = 0$) $[\text{TPyACo}^{\text{III}}(\mathbf{1}_{\text{Cl}}^{2-})\text{Co}^{\text{III}}\text{TPyA}](\text{BF}_4)_4$ ($\mathbf{5}^{4+}$) due to oxidation of $\mathbf{1}_{\text{Cl}}^{3-}$ to $\mathbf{1}_{\text{Cl}}^{2-}$. Formation of the $\mathbf{1}_{\text{Cl}}^{3-}$ radical was also achieved via reduction of $[\text{TPyACo}^{\text{II}}(\mathbf{1}_{\text{Cl}}^{2-})\text{Co}^{\text{II}}\text{TPyA}](\text{BF}_4)_2$ ($\mathbf{5}^{2+}$) to $[\text{TPyACo}^{\text{II}}(\mathbf{1}_{\text{Cl}}^{3-})\text{Co}^{\text{II}}\text{TPyA}](\text{BF}_4)$ ($\mathbf{5}^{3+}$) with $[\text{Co}(\text{C}_5\text{H}_5)_2]$.^[3] $\mathbf{5}^{3+}$ is an example of a valence ambiguous compound, as several reasonable formulations for its electronic structure exist, but the correct formulation is not obvious.

The temperature-dependent magnetic moment, $\mu_{\text{eff}}(T)$, for $\mathbf{5}^{n+}$ ($n = 1, 2, 3$) is presented in Figure 1. $\mathbf{5}^{2+}$ possesses the $\text{Co}^{\text{II}}(\mathbf{1}_{\text{Cl}}^{2-})\text{Co}^{\text{II}}$ core with $S = 3/2$ Co^{II} sites separated by 7.45 Å via a diamagnetic $\mathbf{1}_{\text{Cl}}^{2-}$; hence, only weak antiferromagnetic coupling between the Co^{II} sites is expected and is observed [$J/k_B = -0.65$ K (-0.45 cm $^{-1}$);^[4] $k_B = \text{Boltzmann's constant}$]. Reduction of $\mathbf{5}^{2+}$ to $\mathbf{5}^{3+}$ forms the $\text{Co}^{\text{II}}(\mathbf{1}_{\text{Cl}}^{3-})\text{Co}^{\text{II}}$ core that has a two orders of magnitude enhanced antiferromagnetic coupling [$J/k_B = -75$ K (-52 cm $^{-1}$)] due to the direct exchange coupling between the $S = 3/2$ Co^{II} sites and the $S = 1/2$ $\mathbf{1}_{\text{Cl}}^{3-}$ that links them. In contrast, oxidation of $\mathbf{5}^{2+}$ to $\mathbf{5}^{3+}$ leads to a substantially reduced temperature-independent $\mu_{\text{eff}}(T)$ of 1.75 μ_B that is consistent with one spin per $\mathbf{5}^{3+}$ (Figure 1). In addition, the EPR spectrum of $\mathbf{5}^{3+}$ reveals a Landé g value of 2.0027 that is inconsistent with about 4.3 expected for Co^{II} ,^[5] but characteristic of an organic free radical, that is, $\mathbf{1}_{\text{Cl}}^{3-}$. Thus, the $\mathbf{5}^{3+}$ is assigned the $\text{Co}^{\text{III}}(\mathbf{1}_{\text{Cl}}^{3-})\text{Co}^{\text{III}}$ core. If $\mathbf{5}^{3+}$ had the $\text{Co}^{\text{II}}(\mathbf{1}_{\text{Cl}}^{2-})\text{Co}^{\text{III}}$ electronic structure, it would be expected to have a $\mu_{\text{eff}}(T)$ magnetic behavior characteristic of an $S = 3/2$, $g \approx 4.3$ system, that is, $\mu_{\text{eff}}(T) = 5.68 \mu_B$, which is not observed.



Joel S. Miller is a Distinguished Professor of Chemistry at the University of Utah. He received his B.S. in Chemistry from Wayne State University, Ph.D. from University of California, Los Angeles, and was a postdoctoral associate at Stanford University. After two decades of research at Industrial Laboratories, he joined the University of Utah in 1993. He is interested in the magnetic, electrical, and optical properties of molecule-based materials. He received the 2000 American Chemical Society Award for Chemistry of Materials and the 2007 American Physical Society's McGroddy Prize for New Materials.



Kil Sik Min was born in Sancheong, Republic of Korea. He received his PhD degree from Professor M.P. Suh (Seoul National University, 2000) for research related to functional supramolecules and to magnetic materials. After postdoctoral research stays with Professor Karl Wieghardt (Max-Planck Institute for Bioinorganic Chemistry) and Professor J. S. Miller (University of Utah) since 2002, he joined the Kyungpook National University in 2007. His research interests include the preparation of functional supramolecular compounds and the development of new magnetic materials based on transition metal ions and organic building blocks.

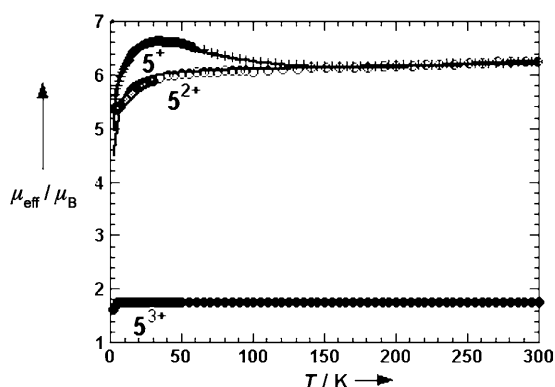


Figure 1. Temperature dependencies of the magnetic moment, $\mu_{\text{eff}}(T)$, for 5^{n+} ($n=1, 2, 3$) (5^{4+} is diamagnetic). Note that the increase in $\mu_{\text{eff}}(T)$ with decreasing temperature below 120 K for 5^+ is suggestive of ferromagnetic coupling. However, as modeled (see text), this is solely due to antiferromagnetic coupling, and several other examples where antiferromagnetic coupling leads to an increase in $\mu_{\text{eff}}(T)$ with decreasing temperature have been reported.^[6]

Infrared spectra also provide information as to the electronic structure of these compounds. The very strong peak at 1526 cm^{-1} is characteristic of the 1_{Cl}^{2-} dianion being present in 5^{2+} . This frequency shifts to 1442 and 1421 cm^{-1} upon either mono-reduction to 5^+ or mono-oxidation to 5^{3+} (Figure 2). This indicates that the 1_{Cl}^{2-} in 5^{2+} is reduced to

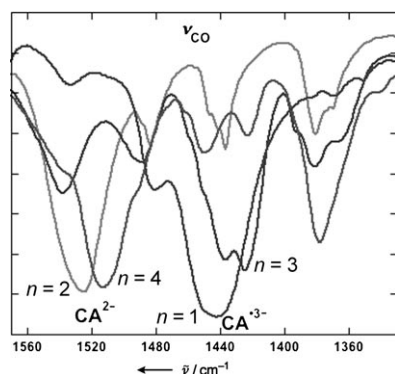


Figure 2. IR spectra for 5^{n+} ($n=1, 2, 3, 4$).

1_{Cl}^{3-} for both 5^+ and 5^{3+} . For 5^{4+} , the strong peak at 1513 cm^{-1} is similar to that observed for 5^{2+} in accord with oxidation of both Co^{II} ions and presence of the 1_{Cl}^{2-} dianion. This circa 90 cm^{-1} shift to lower energy is due to the decreased electron density of the C–O bond, as noted from the two resonance structures for 1_{Cl}^{3-} (Scheme 1).

Although the molecular orbitals of 5^{n+} have not been calculated, insight can be gleaned from the dinuclear ruthenium-based analogue $[(\text{bipy})_2\text{Ru}^{\text{II}}(1_{\text{H}}^{2-})\text{Ru}^{\text{II}}(\text{bipy})_2]^{2+}$ ($\text{bipy} = 2,2'$ -bipyridine). Its HOMO is delocalized over the $\text{Ru}^{\text{II}}(1_{\text{H}}^{2-})\text{Ru}^{\text{II}}$ core with major contributions from both the metal-centered d_{xz} orbitals and π orbitals of the bridging ligand, with 20% of the electron density per ruthenium atom, and the remaining 60% on the bridging 1_{H}^{2-} ligand (Figure 3).^[7] In contrast, its LUMO is primarily located (94%) on the 1_{H}^{2-}



Figure 3. HOMO and LUMO of the $\text{Ru}^{\text{II}}1_{\text{H}}^{2-}\text{Ru}^{\text{II}}$ core of $[(\text{bipy})_2\text{Ru}^{\text{II}}(1_{\text{H}}^{2-})\text{Ru}^{\text{II}}(\text{bipy})_2]^{2+}$. Adapted from reference [7].

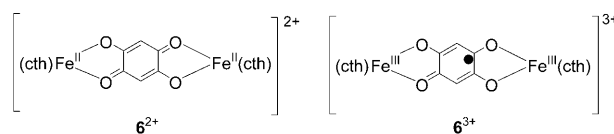
ligand π^* orbital with very small contributions (3%) from each metal d_{xz} orbital. This is in agreement with the EPR data that reveals that the ligand-centered reduced radical is only slightly delocalized onto the metals.^[7] Mono-oxidation formally forms a metal-centered $\text{Ru}^{\text{II}}/\text{Ru}^{\text{III}}$ couple, although it has substantial ligand-based character. There is also a reversible one-electron reduction [$E_{1/2} = -0.63\text{ V}$ (vs. SCE)] that is predominantly ligand-centered. Thus, $[(\text{bipy})_2\text{Ru}^{\text{II}}(1_{\text{H}}^{3-})\text{Ru}^{\text{II}}(\text{bipy})_2]^+$ like $[\text{TPyACo}^{\text{II}}(1_{\text{Cl}}^{3-})\text{Co}^{\text{II}}\text{TPyA}]^+$ (5^+) can be easily formed upon reduction of its dication.

In accord with valence bond resonance (Scheme 1) and MO analyses, the OC–CO bond has less double-bond character for 1_{Cl}^{2-} with respect to 1_{Cl}^{3-} , and is $0.05 \pm 0.02\text{ \AA}$ longer than that observed for 1_{Cl}^{3-} (Figure 4a). In contrast, as noted from the analysis of the IR data above, the C–O bond weakens and is $0.05 \pm 0.02\text{ \AA}$ longer for 1_{Cl}^{3-} with respect to 1_{Cl}^{2-} (Figure 4b).

Hence, the one-electron oxidation of dinuclear complex 5^{2+} leads to a double oxidation and a mono-reduction of the bridging ligand, and is a clear example of a RIET reaction. Crucial is a change in the reduction potential of 1_{Cl}^{3-} bound to two Co^{II} ions upon oxidation of the Co^{II} ions. For 5^{2+} , reduction of 1_{Cl}^{2-} to 1_{Cl}^{3-} requires -0.619 V vs. SCE; however, the 1_{Cl}^{2-} to 1_{Cl}^{3-} reduction occurs in conjunction with the oxidation of Co^{II} going to Co^{III} at $+0.094\text{ V}$. Furthermore, the 1_{Cl}^{3-} to 1_{Cl}^{2-} oxidation reversibly occurs at $+0.619\text{ V}$ for $5^{3+/4+}$.

2.2. Dinuclear Iron and Chromium Tetraoxolene Complexes

Albeit the best characterized, the aforementioned dicobalt complex was not the first reported example of a RIET reaction. Oxidation of $[(\text{cth})\text{Fe}^{\text{II}}(1_{\text{H}}^{2-})\text{Fe}^{\text{II}}(\text{cth})](\text{ClO}_4)_2$ ($\text{cth} = dl\text{-}5,7,7',12,14,14\text{-hexamethyl-}1,4,8,11\text{-tetraazacyclotetradecane}$) (6^{2+}) with AgClO_4 forms $[(\text{cth})\text{Fe}^{\text{III}}(1_{\text{H}}^{3-})\text{Fe}^{\text{III}}(\text{cth})](\text{ClO}_4)_3$ (6^{3+}) via a RIET double oxidation—mono-reduction reaction.^[8] The 6^{3+} core can be formulated as $\text{Fe}^{\text{II}}(1_{\text{H}}^{2-})\text{Fe}^{\text{III}}$, $\text{Fe}^{\text{III}}(1_{\text{H}}^{3-})\text{Fe}^{\text{III}}$, or $\text{Fe}^{\text{II}}(1_{\text{H}}^{3-})\text{Fe}^{\text{II}}$. Its IR and ^{57}Fe Mössbauer spectra, however, indicate that $\text{Fe}^{\text{III}}(1_{\text{H}}^{3-})\text{Fe}^{\text{III}}$ is present, as these spectra are clearly different from that observed for 6^{2+} , and are characteristic of Fe^{III} , whereas evidence for Fe^{II} is not observed. Direct evidence for the presence of 1_{H}^{3-} , however,



(ClO_4)₃ (6^{3+}) via a RIET double oxidation—mono-reduction reaction.^[8] The 6^{3+} core can be formulated as $\text{Fe}^{\text{II}}(1_{\text{H}}^{2-})\text{Fe}^{\text{III}}$, $\text{Fe}^{\text{III}}(1_{\text{H}}^{3-})\text{Fe}^{\text{III}}$, or $\text{Fe}^{\text{II}}(1_{\text{H}}^{3-})\text{Fe}^{\text{II}}$. Its IR and ^{57}Fe Mössbauer spectra, however, indicate that $\text{Fe}^{\text{III}}(1_{\text{H}}^{3-})\text{Fe}^{\text{III}}$ is present, as these spectra are clearly different from that observed for 6^{2+} , and are characteristic of Fe^{III} , whereas evidence for Fe^{II} is not observed. Direct evidence for the presence of 1_{H}^{3-} , however,

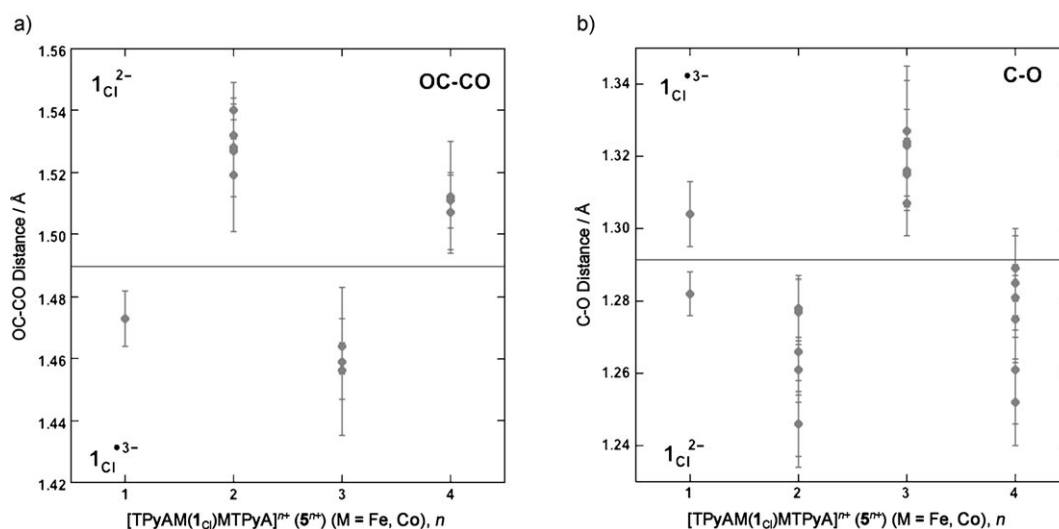


Figure 4. a) OC-CO and b) C-O bond distances for 1_{Cl}^{2-} and 1_{Cl}^{3-} present in 5^{n+} ($n=1, 2, 3, 4$) and $[TPyAFe^{II}1_{Cl}^{2-}Fe^{II}TPyA](BF_4)_2$.^[3] Error bars represent three estimated standard deviations.

was not presented, and 6^{3+} slowly decomposes to mononuclear $[Fe(cth)1_H]^+$.

For 6^{2+} , the magnetic moment of $7.9 \mu_B$ is in accord with two uncoupled high-spin iron(II) ions. In contrast, the moment of 6^{3+} is $9.1 \mu_B$ at room temperature, and increases with decreasing temperature. These data suggest an $S=9/2$ ground state.^[8] The $\mu_{eff}(T)$ data were fit with $J/k_B = -535$ K (-372 cm $^{-1}$) and $g=1.98$, indicating a very strong antiferromagnetic interaction between the Fe^{III} ions and 1_H^{3-} , and a surprisingly low g value.

Similar to 5^{2+} and 5^+ , iron(II) dinuclear complexes, that is, $[TPyAFe^{II}(1_{Cl}^{2-})Fe^{II}TPyA]^{2+}$ and its mono-reduced form $[TPyAFe^{II}(1_{Cl}^{3-})Fe^{II}TPyA]^+$, have been obtained. The very strong peaks at 1524 and 1452 cm $^{-1}$ for $[TPyAFe^{II}(1_{Cl}^{2-})Fe^{II}TPyA]^{2+}$ and $[TPyAFe^{II}(1_{Cl}^{3-})Fe^{II}TPyA]^+$ indicate the presence of 1_{Cl}^{2-} and reduced 1_{Cl}^{3-} , respectively.^[3] Thus, 1_{Cl}^{2-} is reduced to 1_{Cl}^{3-} without reduction of the Fe^{II} ion. Reduction of $[TPyAFe^{II}(1_{Cl}^{2-})Fe^{II}TPyA]^{2+}$ occurs at 0.535 V vs. SCE in reasonable agreement to that observed for 5^{2+} (0.619 V).

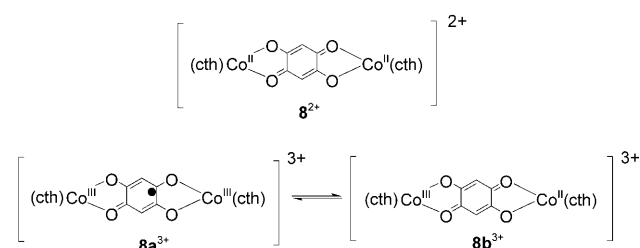
Unusual magnetic behaviors are also observed for $[TPyAFe^{II}(1_{Cl}^{2-})Fe^{II}TPyA]^{2+}$ and $[TPyAFe^{II}(1_{Cl}^{3-})Fe^{II}TPyA]^+$. Like 5^{2+} the former exhibits weak ferromagnetic coupling between the Fe^{II} ions [$g=2.08$, $J/k_B=1.0$ K (0.70 cm $^{-1}$)], while like 5^+ the latter exhibits a significant ferromagnetic interaction between the Fe^{II} ions and the bridging 1_{Cl}^{3-} radical [$J/k_B=28$ K (19.5 cm $^{-1}$), $g=2.03$].^[3,4]

Additionally, the chromium analogue of 6^{3+} , $[(cth)Cr^{III}(1_H^{3-})Cr^{III}(cth)]^{3+}$ (7^{3+}), was formed via the reaction of $Cr^{II}(cth)Cl_2$ with H_21_H .^[8] As its IR spectrum is very similar to that of 6^{3+} , it was proposed to have the same electronic structure. This was supported by a very strong antiferromag-

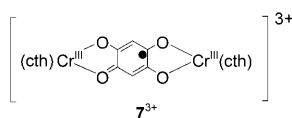
netic interaction [$J/k_B=-393$ K (-273 cm $^{-1}$)] between the Cr^{III} ions and the 1_H^{3-} radical, indicative of the $S=5/2$ ground state for 7^{3+} . This is at variance to the weak antiferromagnetic coupling expected for the $S=2-0-3/2$ mixed-valent $[(cth)Cr^{II}(1_H^{2-})Cr^{III}(cth)]^{3+}$ description, contrary to the spins of the metal ions in $3/2-1/2-3/2$ system. 7^{2+} was not isolated in the synthesis.

2.3. RIET Accompanied by a Valence-Tautomeric Transition

In addition to iron- and chromium-based complexes 6^{3+} and 7^{3+} , the cobalt analogue $[(cth)Co(1_H)Co(cth)](PF_6)_3$ (8^{3+}) was formed from the reaction of $AgNO_3$ and $[(cth)Co^{II}(1_H^{2-})Co^{II}(cth)]^{2+}$ (8^{2+}).



$[(1_H^{2-})Co^{II}(cth)](PF_6)_2$ (8^{2+}). 8^{3+} can be formulated as having a) $Co^{II}1_H-Co^{II}$, b) mixed-valent $Co^{III}1_H^{2-}Co^{II}$, or c) $Co^{III}1_H^{3-}Co^{III}$ cores. The temperature-dependent magnetic susceptibility confirms formulation (c) as the ground state for $8a^{3+}$, but a transition to a higher-moment state occurs at 175 K without thermal hysteresis (Figure 5). This thermally populated excited state is assigned as having the mixed-valence $Co^{III}(1_H^{2-})Co^{II}$ ($8b^{3+}$) dinuclear core (formulation b). Hence, $8a^{3+}$ undergoes a so-called valence tautomeric spin transition at 175 K from the $[(cth)Co^{III}(1_H^{3-})Co^{III}(cth)]^{3+}$ ($8a^{3+}$) ground state to the $[(cth)Co^{III}(1_H^{2-})Co^{II}(cth)]^{3+}$ ($8b^{3+}$) excited state, as verified by IR, EPR, and magnetic



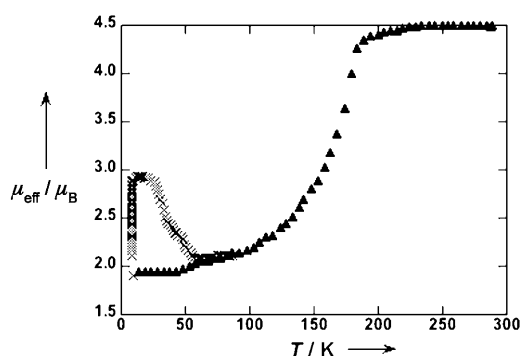
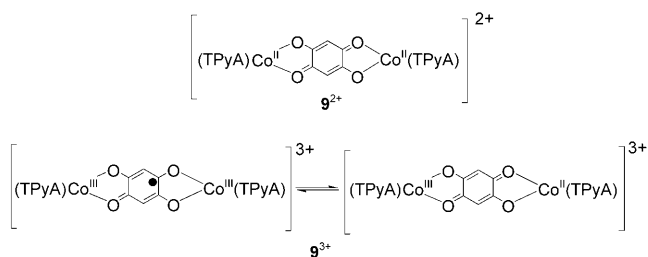


Figure 5. $\mu_{\text{eff}}(T)$ of 8^{3+} measured before (\blacktriangle) irradiation at 647 nm. The crosses indicate the increase of the $\mu_{\text{eff}}(T)$ with time upon irradiation of the sample. Adapted from reference [9].

studies. Hence, unlike 5^{3+} the product of the RIET reaction is itself thermally excited to form the initially anticipated mixed-valent product.

8^{3+} also exhibits photomagnetic effects.^[9] Irradiation of 8^{3+} with 647 nm light leads to an immediate increase of μ_{eff} to circa $3.1 \mu_{\text{B}}$ (Figure 5). After switching off the light, $\mu_{\text{eff}}(T)$ decreases smoothly and at about 60 K μ_{eff} exhibits the initial value obtained prior to irradiation. This light-induced phenomenon is reversible. The level of photoexcitation is circa 40% due to the opacity of the sample.

Similar to 8^{3+} , $[\text{TPyACo}^{\text{III}}(\text{1}_\text{H}^{3-})\text{Co}^{\text{III}}\text{TPyA}](\text{PF}_6)_3$ (9^{3+}) undergoes a transition to the mixed-valent state, but at higher temperature and with thermal hysteresis.^[10] This dicobalt complex exhibits a RIET-related valence tautomeric behav-



ior, that is, $\text{Co}^{\text{III}}(\text{1}_\text{H}^{3-})\text{Co}^{\text{III}} \leftrightarrow \text{Co}^{\text{II}}(\text{1}_\text{H}^{2-})\text{Co}^{\text{III}}$, slightly above room temperature with the transition upon heating occurring at 310 K, and at 297 K upon cooling. Based upon analysis of the magnetic and IR data below 297 K, the dinuclear core of 9^{3+} has the $\text{Co}^{\text{III}}(\text{1}_\text{H}^{3-})\text{Co}^{\text{III}}$ electronic structure, and above it is a mixture of $\text{Co}^{\text{III}}(\text{1}_\text{H}^{3-})\text{Co}^{\text{III}}$ and $\text{Co}^{\text{II}}(\text{1}_\text{H}^{2-})\text{Co}^{\text{III}}$ states. Hence, it has a hysteresis loop that is 13 K wide (Figure 6).

When the 9^{3+} was irradiated with visible light at 5 K for 30 minutes, μ_{eff} increased and reached a saturation value of $2.6 \mu_{\text{B}}$ (Figure 6, inset).^[10] The low efficiency of this photoexcitation is ascribed to the opacity, as reported for 8^{3+} . Reduction of 9^{3+} to 9^{2+} was confirmed by IR spectroscopy, as the peaks at 1530 and 1550 cm^{-1} for 1_H^{2-} increased, while the peak at 1210 cm^{-1} characteristic of 1_H^{3-} decreased. $\mu_{\text{eff}}(T)$ slowly decreased with increasing temperature and at 38 K it reached its initial value. Like 8^{3+} , this light-induced reaction is reversible.

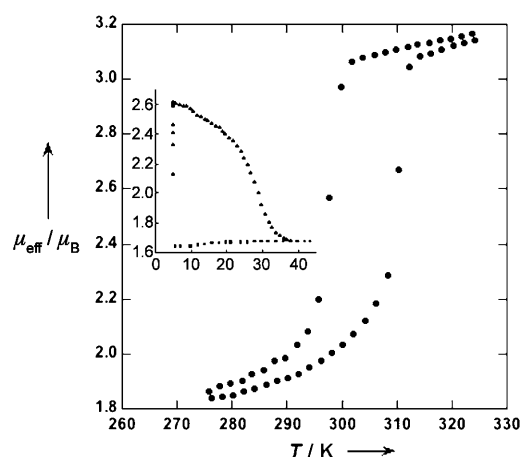
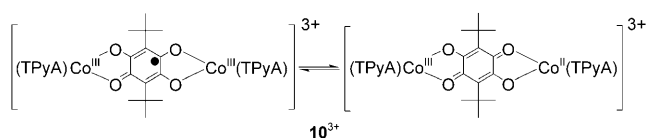


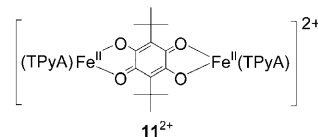
Figure 6. $\mu_{\text{eff}}(T)$ of 9^{3+} and photoinduced changes after irradiation at 532 nm (inset). Adapted from reference [10].

Similar to both 8^{3+} and 9^{3+} , $[\text{TPyACo}^{\text{III}}(\text{1}_\text{Bu}^{3-})\text{Co}^{\text{III}}\text{TPyA}](\text{BF}_4)_3$ (10^{3+}) exhibits a transition around



room temperature, but without thermal hysteresis.^[11] 10^{3+} exhibits a RIET-related valence tautomeric transition, that is, $\text{Co}^{\text{III}}(\text{1}_\text{Bu}^{3-})\text{Co}^{\text{III}} \leftrightarrow \text{Co}^{\text{III}}(\text{1}_\text{Bu}^{2-})\text{Co}^{\text{II}}$, above room temperature. Based upon the analysis of the magnetic, EPR, and IR data, below 300 K the dinuclear core of 10^{3+} has the $\text{Co}^{\text{III}}(\text{1}_\text{Bu}^{3-})\text{Co}^{\text{III}}$ electronic structure, but at higher temperature it is a mixture of $\text{Co}^{\text{III}}(\text{1}_\text{Bu}^{3-})\text{Co}^{\text{III}}$ and $\text{Co}^{\text{III}}(\text{1}_\text{Bu}^{2-})\text{Co}^{\text{II}}$ states similar to 9^{3+} .

It should be noted that several related compounds exhibit spin-crossover behavior.^[12] Spin-crossover behavior arises from thermal population of a metal ion's high-spin electronic structure, and not from a change in the oxidation state of a metal ion, as occurs for valence-tautomeric behavior.^[13] Both behaviors are driven in part by spin entropy, and exhibit an increase, with different degrees of abruptness, in $\mu_{\text{eff}}(T)$ with increasing temperature. This is observed for $[\text{TPyAFe}^{\text{II}}(\text{1}_\text{Bu}^{2-})\text{Fe}^{\text{II}}\text{TPyA}]^{2+}$ (11^{2+}) for which the spin-crossover transition occurs around room temperature (Figure 7).^[14]



2.4. Mixed-Valence Complexes

Valence-ambiguous dinuclear cobalt complexes of the composition $[(\text{triphos})\text{Co}(\text{1}_\text{R})\text{Co}(\text{triphos})]^{n+}$ ($\text{R} = \text{H}, \text{Cl}, \text{Br}, \text{I}, \text{NO}_2, \text{Me}, i\text{Pr}, \text{Ph}$) [$n = 1$ (12^+), 2 (12^{2+}); triphos = 1,1,1-

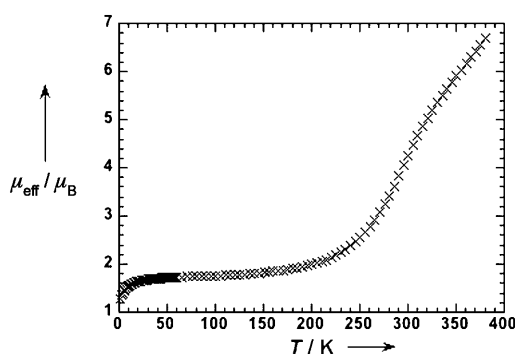
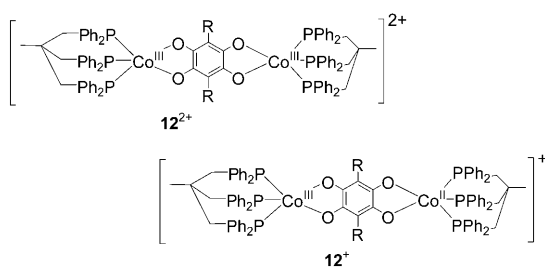


Figure 7. $\mu_{\text{eff}}(T)$ for $[\text{TPyAFe}^{\text{II}}\text{I}_{\text{Bu}}^{2-}\text{Fe}^{\text{II}}\text{TPyA}]^{2+}$ ($\mathbf{11}^{2+}$).^[14]

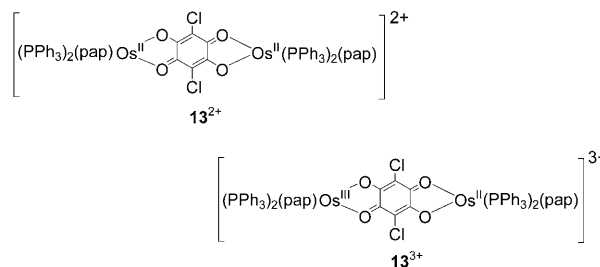


tris(diphenylphosphanomethyl)ethane, $\text{MeC}(\text{CH}_2\text{PPh}_2)_3$ were reported.^[15] Based upon UV/Vis, cyclic voltammetry, NMR, and their structures, $\mathbf{12}^{2+}$ is formulated as $[(\text{triphos})\text{Co}^{\text{III}}(\mathbf{1}_R^{4-})\text{Co}^{\text{III}}(\text{triphos})]^{2+}$, with low-spin Co^{III} ions bridged by the diamagnetic tetraanion, $\mathbf{1}_R^{4-}$. $\mathbf{12}^{2+}$ exhibits two one-electron reduction steps with the separation between reduction waves exceeding 1 V, corresponding to a comproportionation constant for $\text{Co}^{\text{III}}/\text{Co}^{\text{III}} + \text{Co}^{\text{II}}/\text{Co}^{\text{II}} = 2\text{Co}^{\text{III}}/\text{Co}^{\text{II}}$ (i.e. $\mathbf{12}^{2+} + \mathbf{12} = 2\mathbf{12}^+$) cores of about 10^{18} .^[15] $[(\text{triphos})\text{Co}(\mathbf{1}_R)\text{Co}(\text{triphos})]^+$ monocations ($\mathbf{12}^+$; $R = \text{H, Cl, Br, I, Me}$) form from the reduction of $\mathbf{12}^{2+}$ with cobaltocene,^[16] but cannot be isolated due to decomposition upon loss of the solvent and sensitivity to oxygen. Fortunately, $[(\text{triphos})\text{Co}^{\text{III}}(\mathbf{1}_{\text{Cl}}^{4-})\text{Co}^{\text{II}}(\text{triphos})][\text{CoCl}_4]$ ($[\mathbf{12}^+]_2[\text{CoCl}_4]$) is obtained from the reaction of $(\text{triphos})\text{CoCl}$ and $\text{H}_2\mathbf{1}_{\text{Cl}}$ in THF, and the crystal structure has been solved.^[16] All of the mono-reduced monocationic complexes show EPR spectra with $g \approx 2.11$ at 298 K (at 100 K, $g = 2.10$). These g values and the width of the signals indicate a significant unpaired electron density located on the cobalt ions, not on the bridging ligand. The EPR pattern also shows that the electron spin interacts with both cobalt ions; thus, the unpaired electron spin is delocalized over both metal centers on the EPR time scale (10^{-9} s).

Based on cyclic voltammetry, EPR, and UV/Vis data, $\mathbf{12}^{2+}$ is formulated as mixed-valent $[(\text{triphos})\text{Co}^{\text{III}}(\mathbf{1}_R^{4-})\text{Co}^{\text{II}}(\text{triphos})]^+$ ($R = \text{H, Cl, Br, I, Me}$). It exhibits complete electron delocalization indicating that it belongs to Class III of the Robin–Day classification for mixed-valent materials.^[17] With respect to $\mathbf{12}^{2+}$ significant changes in bond length are observed for the Co–O and Co–P bonds for $\mathbf{12}^+$, but the bond lengths of $\mathbf{1}_{\text{Cl}}^{4-}$ ligand remain the same. From analyses of the bond lengths upon mono-reduction of $[(\text{triphos})\text{Co}^{\text{III}}(\mathbf{1}_R^{4-})-$

$\text{Co}^{\text{III}}(\text{triphos})]^{2+}$, one of two cobalt(III) ions is reduced to $[(\text{triphos})\text{Co}^{\text{III}}(\mathbf{1}_{\text{Cl}}^{4-})\text{Co}^{\text{II}}(\text{triphos})]^+$, not the bridging ligand. Thus, the bridging ligand is not involved in the redox reaction. Magnetic data, however, were not reported to further characterize the system.

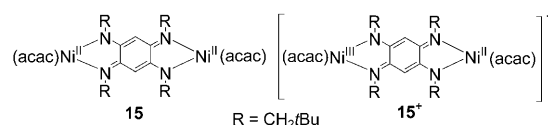
The RIET reaction product observed for the tetraoxolate-based $\mathbf{5}^{3+}$, $\mathbf{6}^{3+}$, $\mathbf{7}^{3+}$, $\mathbf{8}^{3+}$, $\mathbf{9}^{3+}$, and $\mathbf{10}^{3+}$, however, is not observed for the structurally related compounds based on second- and third-row transition metal ions. The one-electron electrochemical oxidation of $[(\text{bipy})_2\text{Os}^{\text{II}}(\mathbf{1}_{\text{Cl}}^{2-})\text{Os}^{\text{II}}(\text{bipy})_2](\text{ClO}_4)_2$,^[18] $[(\text{PPh}_3)_2(\text{pap})\text{Os}^{\text{II}}(\mathbf{1}_{\text{Cl}}^{2-})\text{Os}^{\text{II}}(\text{PPh}_3)_2(\text{pap})](\text{ClO}_4)_2$ [$\text{pap} = 2$ -(phenylazo)pyridine] ($\mathbf{13}^{2+}$),^[18] $[(\text{PPh}_3)_2(\text{CO})_2\text{Os}^{\text{II}}-$



$(\mathbf{1}_{\text{Cl}}^{4-})\text{Os}^{\text{II}}(\text{PPh}_3)_2(\text{CO})_2$],^[18] and $[(\text{bipy})_2\text{Ru}^{\text{II}}(\mathbf{1}_{\text{H}}^{2-})\text{Ru}^{\text{II}}(\text{bipy})_2](\text{PF}_6)_2$ ($\mathbf{14}^{2+}$)^[7] form cations that only exhibit mixed-valent behavior that is attributed to the $\text{M}^{\text{II}}(\mathbf{1}_{\text{Cl}}^{n-})\text{M}^{\text{III}}$ core without formation of a radical-bridging tetraoxolene ligand. It should be noted that the reduced tetraoxolate can be formed upon reduction of $\mathbf{14}^{2+}$ to $[(\text{bipy})_2\text{Ru}^{\text{II}}(\mathbf{1}_{\text{H}}^{3-})\text{Ru}^{\text{II}}(\text{bipy})_2](\text{PF}_6)$ ($\mathbf{14}^+$), in accord with that observed for $\mathbf{5}^{2+}$.

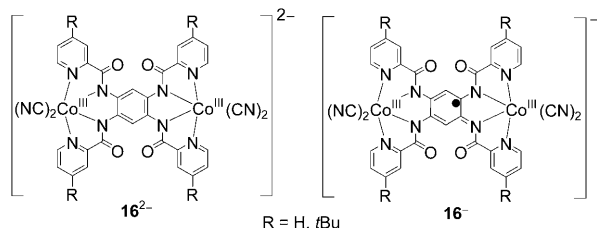
3. Dinuclear Tetraazalene Complexes

In addition to oxygen-donor tetraoxolene bridging ligands, tetraaza-substituted analogues can also exhibit valence-ambiguous behavior. The compound $[(\text{acac})\text{Ni}^{\text{II}}(\text{L}_R^{2-})\text{Ni}^{\text{II}}(\text{acac})]$ ($\mathbf{15}$) [$\text{acac} = \text{acetylacetonate}$; $\text{L} =$



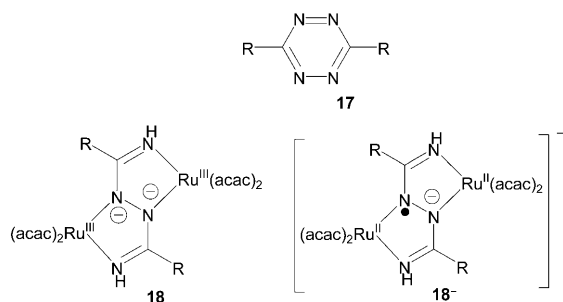
N,N',N'',N''' -tetraeneopentyl-2,5-diamino-1,4-benzoquinonediimine] has been characterized to be diamagnetic.^[19] The 4 K EPR spectrum of the one-electron oxidation species ($\mathbf{15}^+$) has two broad signals corresponding to $g_{\parallel} = 2.13$ and $g_{\perp} = 4.16$ in the presence of a drop of anhydrous pyridine. These values are characteristic of an $S = 3/2$ system in which $S = 1/2 \text{ Ni}^{\text{III}}$ is ferromagnetically coupled to $S = 1 \text{ Ni}^{\text{II}}$. However, at 100 K a $g \approx 2$ signal was observed indicating another coupling mechanism. In the absence of pyridine, a signal at $g = 2.028$ was observed at 4 and 100 K suggesting a strong non-innocent ligand behavior of the bridging ligand, perhaps indicating the presence of $(\text{RN})_4\text{C}_6\text{H}_2^{3-}$.

In contrast to the metal-centered oxidation observed for **15**, ligand-centered oxidations occur for $[\text{N}-(n\text{Bu})_4]_2[(\text{NC})_2\text{Co}^{\text{III}}(\text{tpbp})\text{Co}^{\text{III}}(\text{CN})_2]$ (**16**²⁻) and



$\text{Na}_2[(\text{NC})_2\text{Co}^{\text{III}}(\text{tpb})\text{Co}^{\text{III}}(\text{CN})_2]$ [H_4tpb = 1,2,4,5-tetrakis(2-pyridinecarboxamido)benzene; H_4tpbp = 1,2,4,5-tetrakis(4-*tert*-butyl-2-pyridinecarboxamido)benzene].^[20] In the case of $[(\text{NC})_2\text{Co}^{\text{III}}(\text{tpbp})\text{Co}^{\text{III}}(\text{CN})_2]^{2-}$ (**16**²⁻) the mono-oxidized $[(\text{NC})_2\text{Co}^{\text{III}}(\text{tpbp})\text{Co}^{\text{III}}(\text{CN})_2]^-$ (**16**⁻) species was characterized by coulometry, and its EPR spectrum exhibits a 15-line $S = 1/2$ signal ($g = 2.002$; $A_{\text{Co}} = 15.2$ G) indicative that a bridging radical ligand is present.

The reaction of 3,6-diaryl-1,2,4,5-tetrazine (**17**) and $[\text{Ru}(\text{acac})_2(\text{NCMe})_2]$ results in a reductive tetrazine ring opening to yield $[(\text{acac})_2\text{Ru}^{\text{III}}(\text{dih-R}^{2-})\text{Ru}^{\text{III}}(\text{acac})_2]$ (**18**) [$\text{dih-R}^{2-} = \text{HNC(R)NNC(R)NH}^{2-}$; R = Ph, 2-furyl, 2-thienyl] with a



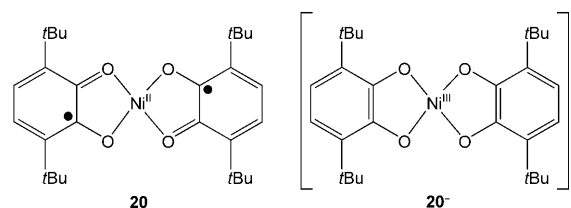
non-innocent 1,2-diiminohydrazido(2-) ligand bridging two ruthenium centers.^[21] The coulometric reduction of **18** forms **18**⁻ that is described as $[(\text{acac})_2\text{Ru}^{\text{II}}(\text{dih-R}^-)\text{Ru}^{\text{II}}(\text{acac})_2]^-$ from an analysis of its EPR spectrum and is in accord with the disappearance of the LMCT band indicating that Ru^{III} is not present. Note that an intense, broad, near-IR absorption at circa 1400 nm can be attributed to an intervalence charge-transfer transition for a mixed-valent $[(\text{acac})_2\text{Ru}^{\text{II}}(\text{dih-R}^-)\text{Ru}^{\text{III}}(\text{acac})_2]^-$ species, and suggests that the mixed-valent configuration is a thermally populated low-lying excited state. Thus, this is an example where a one-electron reduction leads to an oxidation, via two one-electron reductions of two Ru^{III} sites and oxidation of the ligand.

4. Mononuclear Dioxolene Complexes

$[\text{Cr}(o\text{-}t\text{Bu}_2\text{catecholato})_3]^-$ (**19**⁻) was formulated to possess $[\text{Cr}^{\text{V}}(o\text{-}t\text{Bu}_2\text{catecholato}^{2-})_3]^-$, and its one-electron oxidation product was formulated as $[\text{Cr}^{\text{III}}(o\text{-}t\text{Bu}_2\text{semiquinonato}^-)_3]$

(**19**).^[22] Hence, oxidation was thought to lead to reduction of the Cr^{V} to Cr^{III} and oxidation of the three dianionic catechol ligands to their monoanionic semiquinone radical forms. The formal oxidation-state assignment for **19**⁻, however, was reassessed to be $[\text{Cr}^{\text{III}}(o\text{-}t\text{Bu}_2\text{semiquinonato}^-)_2(o\text{-}t\text{Bu}_2\text{catecholato}^{2-})]^-$.^[23] Thus, oxidation leads only to ligand-based oxidations. Cobalt analogues frequently exhibit valence-tautomeric behavior in accord with this observation.^[13]

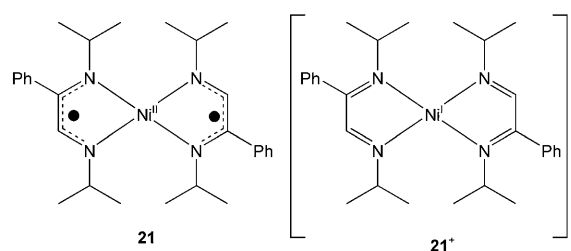
Reduction of $[\text{Ni}^{\text{II}}(3,6\text{-dbsq})_2]$ (dbsq = 3,6-di-*tert*-butyl-1,2-benzosemiquinonate) (**20**) with cobaltocene forms



20⁻.^[24] **20**⁻ exhibits an anisotropic EPR spectrum typical of Ni^{III} with $g_1 = 1.998$, $g_2 = 2.015$, and $g_3 = 2.121$. Hence, **20**⁻ is described as $(\text{CoCp}_2)[\text{Ni}^{\text{III}}(3,6\text{-DBCat})_2]$, and, thus, results from a RIET reaction whereby two one-electron reductions a metal-centered oxidation occurs.

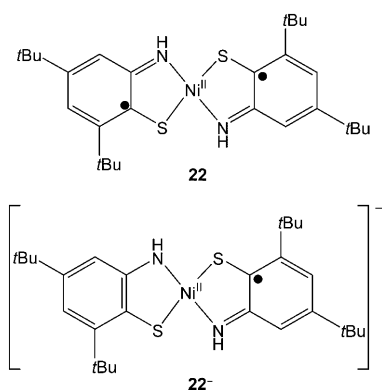
5. Mononuclear Tetraazalene Complexes

Very recently $[\text{Ni}^{\text{II}}(\text{L}^-)_2]$ [L = 2-phenyl-1,4-bis(isopropyl)-1,4-diazabutadiene] (**21**) was prepared and formulated to



possess a tetrahedrally coordinated Ni^{II} with two chelating radical anionic ligands.^[25] The one-electron oxidation of **21** with ferrocenium forms **21**⁺, which has a tetrahedral one-electron-reduced Ni^{I} central ion, and one-electron oxidations of both L^- to L . Hence, oxidation leads to reduction of Ni^{II} to Ni^{I} with the concomitant oxidation of the ligand.

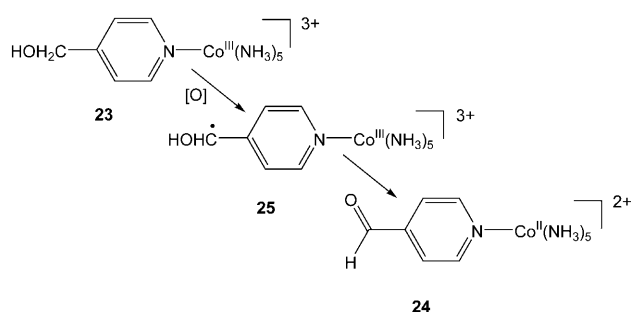
The coulometric reduction product of $[\text{Ni}^{\text{II}}(\text{L}^{\text{isq}})_2]$ ($\text{L}^{\text{isq}} = 2,4\text{-di-}t\text{-butyl-6-iminothionebenzosemiquinonate}$) (**22**) can be formulated as either $[\text{Ni}^{\text{I}}(\text{L}^{\text{isq}})_2]^-$, $[\text{Ni}^{\text{II}}(\text{L}^{\text{ap-H}})(\text{L}^{\text{isq}})]^-$ or $[\text{Ni}^{\text{III}}(\text{L}^{\text{ap-H}})_2]^-$ ($\text{L}^{\text{ap}} = 2,4\text{-di-}t\text{-butyl-6-aminothiophenolate}$).^[26] with the latter formulation being a consequence of a RIET reaction. Although **22**⁻ has not been isolated as a pure solid, its EPR ($g_1 = 2.0055$, $g_2 = 2.0282$, and $g_3 = 2.1147$) and



UV/Vis spectra and DFT calculations led to the assignment of **22**[−] as [Ni^{II}(L^{ap}-H)(L^{sq})][−]; hence, this is not a RIET reaction. Nonetheless, **22**[−] is comparable to **20**[−] where a RIET reaction is evident (for example, comparable EPR spectra). Unfortunately, crystallographic data to confirm this assignment has not been presented, and a more detailed analysis of **22**[−] and **20**[−] is warranted to confirm their respective electronic structures.

6. Chemical Reactions

The one-electron chemical oxidation of [Co(NH₃)₅(1,4-NC₅H₄CH₂OH)]³⁺ (**23**) with, for example, Ce^{IV} or S₂O₈^{2−},

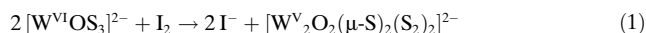


forms products consistent with the formation of labile **24**, indicative of an oxidation-induced electron-transfer reaction. The initial one-electron oxidation was proposed to oxidize the -CH₂OH group to the -CHOH (**25**) radical that, via an internal electron rearrangement, is further oxidized to an aldehyde while the Co^{III} site is reduced to Co^{II} (**24**).^[27] Hence, oxidation leads to reduction of the metal ion.

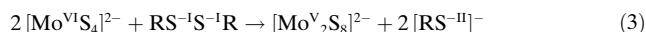
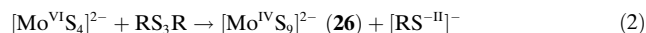
RIET reactions have also been established to occur for several examples of metal complexes with S-based ligands whereby both a) oxidation leading to reduction of the metal site and oxidation of the S-based ligand, and b) reduction leading to oxidation of the metal site and reduction of the S-based ligand can occur.^[28] Note that these reactions differ from that reported for **5**³⁺–**10**³⁺, as RIET is a net effect from the overall chemical reaction, which frequently have other reactants or products. The detailed mechanistic pathways for these complex redox reactions are unknown. In contrast, **5**³⁺–

10³⁺ involve the consequences of a single loss of an electron per molecule.

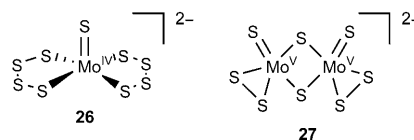
Examples of this class of reactions include the iodine oxidation of [W^{VI}OS₃]^{2−} to [W^V₂O₂(μ-S)₂(S₂)₂]^{2−}, which is best described as [W^V₂O₂(μ-S)₂(S₂)₂]^{2−} [Eq. (1)].^[29]



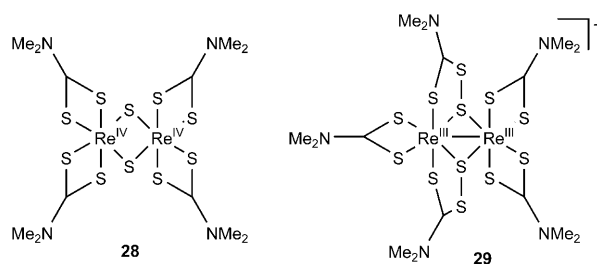
Further examples are given in Equations (2) and (3), where the structure [Mo^{IV}S₉]^{2−} in Equation (2) is really [S=Mo^{IV}(S₄)₂]^{2−} (**26**).^[30]



Assignment of the local oxidation states required the determination of the structure of [Mo^V₂S₈]^{2−}, which reveals the dianion to be [Mo^V₂(μ-S^{2−})₂(S^{2−})₂(S₂^{2−})₂]^{2−} (**27**).^[31] Hence,



for **27** oxidation leads to S^{2−}-oxidation to S₂^{2−} in addition to reduction of Mo^{VI} to Mo^V. Similarly, the RIET reactions of [M^{VI}S₄]^{2−} (M = Mo, W) and bis(trifluoromethyl)-1,2-dithiete forms [M^{IV}(S₂C₂(CF₃)₂)₃]^{2−},^[32] and [V^VS₄]^{3−} and [tBuNCs₂]₂ forms [V^{IV}₂(μ-S₂^{2−})(S₂NtBu₂)₄]^{3−}.^[33] Likewise, the reaction of [Re^{IV}S₄][−] and a) [Me₂NC(S)S]₂ forms [Re^{IV}₂(μ-S)₂(S₂CNMe₂)₄] (**28**),^[34] b) [PhCS₂]₂ forms [Re^{III}₂(S₂CPh)₂(S₂CPh)₂]^{3−},^[35] and c) [nBuOCS₂]₂ forms [Re^{IV}₂(μ-S)₂(S₂CONtBu)₃][−].^[36] In contrast, LiBEt₃H reduction of [Re^{III}₂(μ-S₂CNMe₂)₂(S₂CNMe₂)₃]⁺ (**29**) also forms [Re^{IV}₂(μ-S)₂(S₂CNMe₂)₄] (**28**).^[37] Thus, reduction of **29** leads to S₂NMe₂[−] reduction, and oxidation of Re^{III} to Re^{IV}.



7. Biological Systems

RIET has been noted to occur in a few, but important, biological reactions, namely the reduction of cytochrome *b* upon aerial oxygen, and with Ni-Fe hydrogenase. The reduction of cytochrome *b* upon addition of oxygen has been discussed by Chance^[38] and Wilson et al.^[39] The midpoint potential of cytochrome *b*₅₆₆ was raised by about 0.275 V after the addition of ATP. Hence, this required activation of

electron transport through cytochrome c_1 , and an energy-dependent change in the midpoint-potential of cytochrome b_{566} , is a consequence of activation of the electron transfer. The rapid reducibility of cytochrome b_{566} observed in the presence of antimycin A was ascribed to an increase in the midpoint potential of the cytochrome, and the aerobic reduction of cytochrome b_{566} depends on the oxidation of cytochrome c , as well as donation of another electron donor to cytochrome b_{566} .

In Ni-Fe hydrogenase the detailed reaction mechanism is still controversial due to the ambiguity of the redox states involved in the one-electron reduction of the active site via a two-electron redox process.^[40] Aerobic Ni-Fe hydrogenase has two catalytically inactive forms, as identified from different EPR signals: Form A [Ni-A unready form, $\text{Ni}^{\text{III}}_{\text{ls}}\text{-Fe}^{\text{II}}_{\text{ls}}$ ($g = 2.31, 2.23$, and 2.02)] and Form B [Ni-B ready form, $\text{Ni}^{\text{III}}_{\text{ls}}\text{-Fe}^{\text{II}}_{\text{ls}}$ ($g = 2.33, 2.16$, and 2.01)]. Form B (Ni-B) is rapidly reduced by H_2 , whereas Form A (Ni-A) is only activated by hydrogen over several hours. The reduction of Forms A and B are accompanied by the uptake of one electron, and simultaneously the EPR signal disappears, giving rise to an EPR-silent intermediate redox level, SI. Form SI_a is in redox equilibrium with Form A, while Form SI_r is in redox equilibrium with Form B, and Form SI_c is in redox equilibrium with Form C. Each reduction process is associated with the uptake of one electron and one proton by the enzyme. Form SI_r is in equilibrium with Form SI_a , which is the SI state through which the more reduced forms of the enzyme are accessed. These reduced forms include the EPR-active Form C and the EPR-silent fully reduced Form R. The one-electron reduction of SI produces Form C. The nickel center in Form C can be formulated as either $\text{d}^9 \text{Ni}^{\text{I}}$ or $\text{d}^7 \text{Ni}^{\text{III}}$.

In the case of $\text{d}^9 \text{Ni}^{\text{I}}$, the redox chemistry associated with the reductive activation of the enzyme is $\text{Ni}^{\text{III}} \rightarrow \text{Ni}^{\text{II}} \rightarrow \text{Ni}^{\text{I}}$ suggestive of a major structural change in the active site, as the $\text{Ni}^{\text{III/II}}$ and $\text{Ni}^{\text{II/I}}$ redox couples are more than 2 V apart in model systems, but are assigned to a difference of less than 0.2 V in the enzyme. Alternatively, a redox oscillation mechanism involving $\text{Ni}^{\text{III}} \rightarrow \text{Ni}^{\text{II}} \rightarrow \text{Ni}^{\text{III}}$ redox states consistent with the EPR spectra may occur. In this scheme, all of the EPR-active species would be formally low-spin $\text{d}^7 \text{Ni}^{\text{III}}$ species.^[39,41] Recent studies of the redox chemistry of Form C indicate a redox oscillation mechanism is most consistent with the data.^[42] Thus, the nickel center in Form C can be considered as Ni^{III} . In the reaction step, an electron is added to the SI_a form [that is, $\text{Ni}^{\text{II}}\text{-Fe}^{\text{II}}$] of the enzyme leading to an oxidized $\text{Ni}^{\text{III}}\text{-Fe}^{\text{II}}$ form. That is, the reduction of the enzyme induces the oxidation of the nickel center of the active site. This unusual reaction is involved in an addition of proton of enzyme to give rise to hydride.

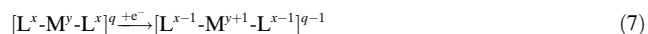
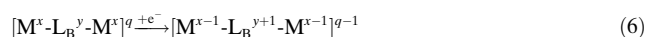
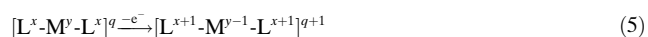
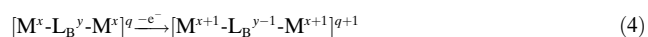
8. Theoretical Considerations

The theoretical basis for RIET reactions is far from established. Recently, a paper with the provocative title “Can one oxidize an atom by reducing the molecule that contains it?”^[43a] was brought to our attention.^[43c] In this paper Ayers identifies mathematical conditions necessary for the title to be

valid; namely, that three redox active sites must be present (as occurs for $4^{3+}\text{-}10^{3+}$), and that the system must be described by a negative condensed Fukui function. The condensed Fukui function measures how many electrons within an atom-in-a-molecule are gained (or lost) upon reduction (or oxidation) and is typically positive. The negative value required for a RIET reaction to occur is a consequence of an orbital relaxation effect.^[43a,b] More detailed theoretical insight is essential to understand the conditions and requirements to utilize and design new materials that undergo either reduction upon oxidation, or oxidation upon reduction, and further studies are essential to elucidate the mechanism, and understand the nuances and limitations of these complex redox reactions.

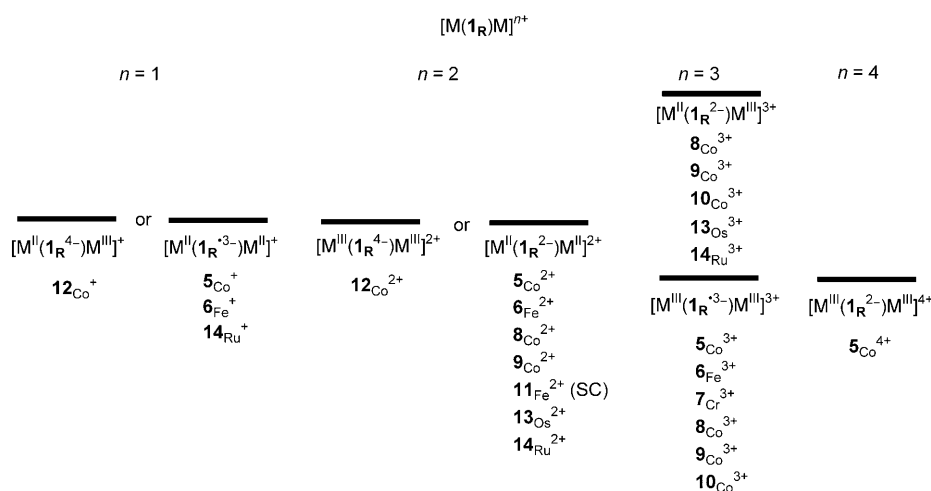
9. Summary and Outlook

RIET examples have been characterized whereby an oxidation leads to a reduction (as well as a reduction that leads to an oxidation). In reality, these reactions are respectively two one-electron oxidations and a one-electron reduction (or two one-electron reductions and a one-electron oxidation). These are summarized via the generalized formulas (4) and (5) for oxidation leading to reduction of Type 2 and 3 species, respectively, and (6) and (7) for reduction leading to oxidation of Type 2 and 3 species, respectively.



This RIET reaction can lead to complex chemical processes that impact chemical synthesis as well as biological and physical processes, and may well play a role in catalysis, and future electronic display devices etc. The best-characterized materials are based upon dinuclear metal complexes with bridging tetraoxolate ligands, **2** and **4**, and are the focal point of this Minireview, although examples of a single metal ion possessing two non-innocent chelating ligands (**3**) have been reported. Hence, the presence of three redox-active sites appears essential, but is insufficient, in accord with a theoretical perspective.^[43] Further examples as well as extension of these structural types undoubtedly will be rewarded with exotic materials and phenomena.

Dinuclear structures (**2** and **4**) possessing the $[\text{M}\mathbf{1}_R\text{M}]^{n+}$ core are valence ambiguous and can possess several electronic states (Scheme 2), which in some cases can be thermally (and photochemically) altered. The electronic structure for $n = 2$ is typically $[\text{M}^{\text{II}}\mathbf{1}_R^{2-}\text{M}^{\text{II}}]^{2+}$, as observed for $\text{M} = \text{Co}, \text{Fe}, \text{Ru}, \text{Os}$; however, $[\text{M}^{\text{III}}\mathbf{1}_R^{4-}\text{M}^{\text{III}}]^{2+}$ occurs for $\text{M} = \text{Co}$ with strong-field triarylphosphine-based ancillary ligands. Spin-crossover behavior has been observed for $\text{M} = \text{Fe}$. Oxidation to $[\text{M}\mathbf{1}_R\text{M}]^{3+}$ can form the mixed-valent $[\text{M}^{\text{II}}\mathbf{1}_R^{2-}\text{M}^{\text{III}}]^{3+}$ electronic structure, as reported for $\text{M} = \text{Ru}$. For $\text{M} = \text{Co}, \text{Cr}$, and Fe , however, this mixed-valent formulation is not the ground



Scheme 2.

state. Instead, the RIET $[M^{III}1_R^{3-}M^{III}]^{3+}$ electronic structure frequently has the lowest energy. For some dinuclear cobalt complexes the mixed-valent $[M^{II}1_R^{2-}M^{III}]^{3+}$ electronic state can be thermally populated with depopulation of the RIET product $[M^{III}1_R^{3-}M^{III}]^{3+}$ ground electronic state. Further oxidation to $n=4$ leads to the $[M^{III}1_R^{2-}M^{III}]^{4+}$ electronic structure. Reduction of $[M^{II}1_R^{2-}M^{II}]^{2+}$ forms either $[M^{II}1_R^{3-}M^{II}]^+$ when it possesses the $[M^{II}1_R^{2-}M^{II}]^{2+}$ electronic structure, or $[M^{II}1_R^{4-}M^{III}]^+$ when it possesses the $[M^{III}1_R^{4-}M^{III}]^{2+}$ electronic structure. These RIET reactions are limited to the first-row transition metals chromium, iron, and cobalt; however, with a different non-innocent bridging ligand it has been observed for second-row ruthenium. Thus, RIET reactions strongly depend on the bridging and/or peripheral ligands, and are not restricted to a few elements.

Examples of mononuclear materials possessing two redox active (non-innocent) ligands (20^- and 21^+) such that the RIET reaction occurs has been clearly established, but several others have been challenging to characterize unambiguously. $[Cr(o-tBu_2catecholato)_3]^-$ (19^-) is best described as the non-RIET $[Cr^{III}(o-tBu_2semiquinonato^-)_2(o-tBu_2catecholato^{2-})]^-$, although it was initially formulated as a RIET product. Clearly anticipating of electron transfer related to RIET reactions, as well as their detailed characterization, is challenging, and more examples displaying a RIET are required.

With the identification of model compounds exhibiting RIET, more detailed theoretical insights are anticipated in the future. These insights should lead to new families of materials, which may have applications in sensors, devices, and actuators of the future. Undoubtedly RIET reactions may be more common in larger polynuclear cluster and biological systems, and further studies of biologically important reactions should provide insight into the importance of RIET in biologically important processes. Furthermore, new materials extending the range of properties, ideally to include the presence of spin crossover behavior in addition to valence tautomeric behavior are anticipated in the future.

The authors gratefully acknowledge numerous helpful discussions with Paul W. Ayers (McMaster University), Brian R. Gibney (Columbia University), Eric L. Hegg (Michigan State University), Roald Hoffmann (Cornell University), Jason Schaller, William W. Shum, and Henry S. White, and the continued partial support by the U.S. Department of Energy Division of Material Science (Grant No. DE-FG03-93ER45504 and DE-FG02-01ER45931) and U.S. Air Force Office of Scientific Research (Grant No. F49620-03-1-0175).

Received: November 7, 2007

Revised: February 25, 2008

Published online: October 29, 2008

- a) *Encyclopedia of Electrochemistry of the Elements* (Ed.: A. J. Bard), Marcel Dekker, New York, **1986**; b) D. H. Evans, *Chem. Rev.* **1990**, *90*, 739; c) H. Taube, E. S. Gould, *Acc. Chem. Res.* **1969**, *2*, 321; d) V. L. Davidson, *Acc. Chem. Res.* **2000**, *33*, 87.
- M. D. Ward, J. A. McCleverty, *J. Chem. Soc. Dalton* **2002**, 275; C. K. Jørgenson, *Coord. Chem. Rev.* **1966**, *1*, 164.
- K. S. Min, A. G. DiPasquale, J. A. Golen, A. L. Rheingold, J. S. Miller, *J. Am. Chem. Soc.* **2007**, *129*, 2360.
- All J values reported herein are based on the Hamiltonian: $H = -2J S_a S_b$.
- A. Sokolowski, B. Adam, T. Weyhermüller, A. Kikuchi, K. Hildenbrand, R. Schnepf, P. Hildebrandt, E. Bill, K. Wieghardt, *Inorg. Chem.* **1997**, *36*, 3702.
- Y. Pei, Y. Journaux, O. Kahn, A. Dei, D. Gatteschi, *J. Chem. Soc. Chem. Commun.* **1986**, 1300; Y. Pei, Y. Journaux, O. Kahn, *Inorg. Chem.* **1988**, *27*, 399; P. Chaudhuri, M. Winter, P. Fleischhauer, W. Haase, U. Flörke, H.-J. Haupt, *J. Chem. Soc. Chem. Commun.* **1990**, 1728.
- M. D. Ward, *Inorg. Chem.* **1996**, *35*, 1712.
- A. Dei, D. Gatteschi, L. Pardi, U. Russo, *Inorg. Chem.* **1991**, *30*, 2589.
- C. Carbonera, A. Dei, J.-F. Letard, C. Sangregorio, L. Sorace, *Angew. Chem.* **2004**, *116*, 3198; *Angew. Chem. Int. Ed.* **2004**, *43*, 3136.
- J. Tao, H. Maruyama, O. Sato, *J. Am. Chem. Soc.* **2006**, *128*, 1790.
- K. S. Min, J. S. Miller, unpublished results.
- Spin Crossover in Transition Metal Compounds*, Vols. 1, 2 and 3 (Eds.: P. Gülich, H. A. Goodwin), Springer, Berlin, **2004**.
- D. A. Shultz in *Magnetism—Molecules to Materials*, Vol. 2 (Eds.: J. S. Miller, M. Drillon), Wiley-VCH, Weinheim, **2001**, p. 281; G. C. Pierpont, R. M. Buchanan, *Coord. Chem. Rev.* **1981**, *38*, 45; C. C. G. Pierpont, C. W. Lange, *Prog. Inorg. Chem.* **1994**, *41*, 331.
- K. S. Min, A. G. DiPasquale, A. L. Rheingold, J. S. Miller, *Inorg. Chem.* **2007**, *46*, 1048.
- K. Heinze, G. Huttner, L. Zsolnai, A. Jacobi, P. Schöber, *Chem. Eur. J.* **1997**, *3*, 732.
- K. Heinze, G. Huttner, O. Walter, *Eur. J. Inorg. Chem.* **1999**, 593.
- M. B. Robin, P. Day, *Adv. Inorg. Chem. Radiochem.* **1967**, *10*, 247.
- P. Gupta, A. Das, F. Basuli, A. Castineiras, W. S. Sheldrick, H. Mayer-Figge, S. Bhattacharya, *Inorg. Chem.* **2005**, *44*, 2081.

- [19] O. Siri, J.-P. Taquet, J.-P. Collin, M.-M. Rohmer, M. Bénard, P. Braunstein, *Chem. Eur. J.* **2005**, *11*, 7247.
- [20] U. Beckmann, E. Bill, T. Weyhermüller, K. Wieghardt, *Inorg. Chem.* **2003**, *42*, 1045.
- [21] S. Maji, B. Sarkar, S. Patra, J. Fiedler, S. M. Mobin, V. G. Puranik, W. Kaim, G. K. Lahiri, *Inorg. Chem.* **2006**, *45*, 1316.
- [22] A. Levina, G. J. Foran, D. I. Pattison, P. A. Lay, *Angew. Chem.* **2004**, *116*, 468; *Angew. Chem. Int. Ed.* **2004**, *43*, 462; D. I. Pattison, A. Levina, H. H. Harris, P. Turner, P. A. Lay, *Inorg. Chem.* **2001**, *40*, 214; C. Milsman, A. Levina, G. J. Foran, D. I. Pattison, P. A. Lay, *Inorg. Chem.* **2006**, *45*, 4743.
- [23] C. Pierpont, *Inorg. Chem.* **2001**, *40*, 5727; R. R. Kapre, E. Bothe, T. Weyhermüller, S. D. George, N. Muresan, K. Wieghardt, *Inorg. Chem.* **2007**, *46*, 78727.
- [24] C. W. Lange, C. G. Pierpont, *Inorg. Chim. Acta* **1997**, *263*, 219.
- [25] N. Muresan, K. Chlopek, T. Weyhermüller, F. Neese, K. Wieghardt, *Inorg. Chem.* **2007**, *46*, 5327.
- [26] D. Herebian, E. Bothe, E. Bill, T. Weyhermüller, K. Wieghardt, *J. Am. Chem. Soc.* **2001**, *123*, 10012.
- [27] H. Taube, *Electron Transfer Reactions of Complex Ions in Solution*, Academic Press, NY, **1970**, p. 73–98.
- [28] M. A. Harmer, T. L. Halbert, W.-H. Pan, C. L. Coyle, S. A. Cohen, E. I. Stiefel, *Polyhedron* **1986**, *5*, 341.
- [29] S. Sarkar, M. A. Ansari, *J. Chem. Soc. Chem. Commun.* **1986**, 324.
- [30] E. D. Simhon, N. C. Baenziger, M. Kanatzidis, D. Coucouvanis, *J. Am. Chem. Soc.* **1981**, *103*, 1218; M. Draganjac, E. Simhon, L. T. Chan, M. Kanatzidis, N. C. Baenziger, D. Coucouvanis, *Inorg. Chem.* **1982**, *21*, 3321.
- [31] W.-H. Pan, M. A. Harmer, T. L. Halbert, E. I. Stiefel, *J. Am. Chem. Soc.* **1984**, *106*, 459.
- [32] K. Wang, J. M. McConnachie, E. I. Stiefel, *Inorg. Chem.* **1999**, *38*, 4334.
- [33] T. L. Halbert, L. L. Hutchings, R. Rhodes, E. I. Stiefel, *J. Am. Chem. Soc.* **1986**, *108*, 6437.
- [34] H. H. Murray, L. Wei, S. E. Sherman, M. A. Greaney, K. A. Eriksen, B. Cartensen, T. L. Halbert, E. I. Stiefel, *Inorg. Chem.* **1995**, *34*, 841.
- [35] C. A. McConnachie, E. I. Stiefel, *Inorg. Chem.* **1997**, *38*, 6144.
- [36] C. A. McConnachie, E. I. Stiefel, *Inorg. Chem.* **1999**, *36*, 964.
- [37] L. Wei, T. L. Halbert, H. H. Murray, III, E. I. Stiefel, *J. Am. Chem. Soc.* **1990**, *112*, 6431.
- [38] M. Erecinska, B. Chance, D. F. Wilson, P. L. Dutton, *Proc. Natl. Acad. Sci. USA* **1972**, *69*, 50.
- [39] D. F. Wilson, P. L. Dutton, *Biochem. Biophys. Res. Commun.* **1970**, *39*, 59.
- [40] M. J. Maroney, P. A. Bryngelson, *J. Biol. Inorg. Chem.* **2001**, *6*, 453.
- [41] M. Teixeira, I. Moura, A. V. Xavier, B. H. Huynh, D. V. Der Vartanian, H. D. Peck, J. LeGall, J. J. G. Moura, *J. Biol. Chem.* **1985**, *260*, 8942.
- [42] G. Davidson, S. B. Choudhury, Z. Gu, K. Bose, W. Roseboom, S. P. J. Albracht, M. J. Maroney, *Biochemistry* **2000**, *39*, 7468.
- [43] a) P. W. Ayers, *Phys. Chem. Chem. Phys.* **2006**, *8*, 3387; b) P. W. Ayers, private communication; c) R. Hoffmann kindly provided this reference.